

## Mitochondrial dysfunction as an early event in the process of apoptosis induced by woodfordin I in human leukemia K562 cells

Ming-Jie Liu,<sup>a</sup> Zhao Wang,<sup>a,\*</sup> Hai-Xia Li,<sup>b</sup> Rong-Cong Wu,<sup>a</sup> Yan-Ze Liu,<sup>b</sup> and Qing-Yu Wu<sup>a</sup>

<sup>a</sup>Department of Biological Sciences and Biotechnology, Tsinghua University, Beijing 100084, PR China

<sup>b</sup>Department of Phytochemistry, He'nan College of Traditional Chinese Medicine, Zhengzhou, PR China

Received 7 June 2003; accepted 25 August 2003

### Abstract

Tannins are a group of widely distributed plant polyphenols, some of which are beneficial to health because of their chemopreventive activities. In the present study, we investigated the effects and action mechanisms of woodfordin I, a macrocyclic ellagitannin dimer, on human chronic myelogenous leukemia (CML) K562 cells. The results showed that woodfordin I was able to suppress the proliferation and induce apoptosis in K562 cells. Apoptosis was evaluated by cytomorphology, internucleosomal DNA fragmentation, and externalization of phosphatidylserine. Woodfordin I treatment caused a rapid and sustained loss of mitochondrial transmembrane potential (MMP), transient generation of reactive oxygen species (ROS), transient elevation of intracellular  $Ca^{2+}$  concentration, and cytosolic accumulation of cytochrome *c*. The activation of caspase-9 and 3, but not caspase-8, was also demonstrated, indicating that the apoptotic signaling triggered by woodfordin I was mediated through the intrinsic mitochondria-dependent pathway. Western blot and immunofluorescence analysis revealed that the anti-apoptotic Bcl-2 and Bcl-x<sub>L</sub> levels were downregulated, together with the pro-apoptotic Bax protein. Significantly, woodfordin I-induced apoptosis was associated with a decline in the levels of c-Abl, Bcr-Abl, and cellular protein tyrosine phosphorylation. Considering the consequence of all the events in the process of woodfordin I-induced apoptosis, the mitochondrial dysfunction is directly responsible for the pro-apoptotic effects on K562 cells. Furthermore, because CML is a malignancy of pluripotent hematopoietic cells caused by the dysregulated tyrosine kinase activity of Bcr-Abl, these findings suggest that woodfordin I may be a potential lead compound against CML.

© 2003 Elsevier Inc. All rights reserved.

**Keywords:** Woodfordin I; Apoptosis; Tannins; Mitochondria; Bcr-Abl; Bcl-x<sub>L</sub>; K562 cells

### Introduction

Plant tannins represent one of the most ubiquitous groups of natural polyphenols. Researchers' interests in these somewhat structurally diverse secondary metabolites are heightened by their profound health-beneficial properties in certain beverages and by their identification as the principle curative agents in a variety of traditional herbal medicine. Recent studies have determined a lot of pure tannins with significant biological and pharmacological activities, such as antimicrobial (Burapadaja and Bunchoo, 1995), antiviral (Nakashima et al., 1992), antioxidant (Satoh and Sakagami, 1996), and antitumor activities (Gali et al., 1992; Miyamoto et al., 1993a; Mukhtar et al., 1988). Classically, tannins are divided into two chemically distinct groups: the condensed tannins, also referred to as proanthocyanidins, and the hydrolyzable tannins. Of special interest is the rigid structure of the

hydrolyzable macrocyclic ellagitannins, such as woodfordin C (Kuramochi-Motegi et al., 1992), oenothin B (Miyamoto et al., 1993b) and camelliin B (Yoshida et al., 1989), which exhibit inherently low cytotoxicity and potent antitumor activity. Woodfordin I was isolated from a traditional Chinese medicine, *Chamaenerion angustifolium* (L.) Scop. The unique structure is characterized as a macrocyclic ellagitannin dimer (Yoshida et al., 1992), indicating its potential biological activity (Fig. 1).

Apoptosis is essential for normal development and the maintenance of homeostasis. It is a highly regulated cellular process with characteristic morphological and biochemical features. Caspases are a highly conserved cysteine protease family and involved in both commitment and execution phases of apoptosis, resulting in cleavage of specific substrate proteins (Sakahira et al., 1998; Thornberry et al., 1997). Two major apoptotic signaling pathways have been defined. The mitochondria-dependent pathway is responsible for extracellular cues and internal insults such as DNA damage. Cytotoxic stress causes pro-apoptotic members of the Bcl-2 family, such

\* Corresponding author. Fax: +86-10-62772240.

E-mail address: [zwang@tsinghua.edu.cn](mailto:zwang@tsinghua.edu.cn) (Z. Wang).

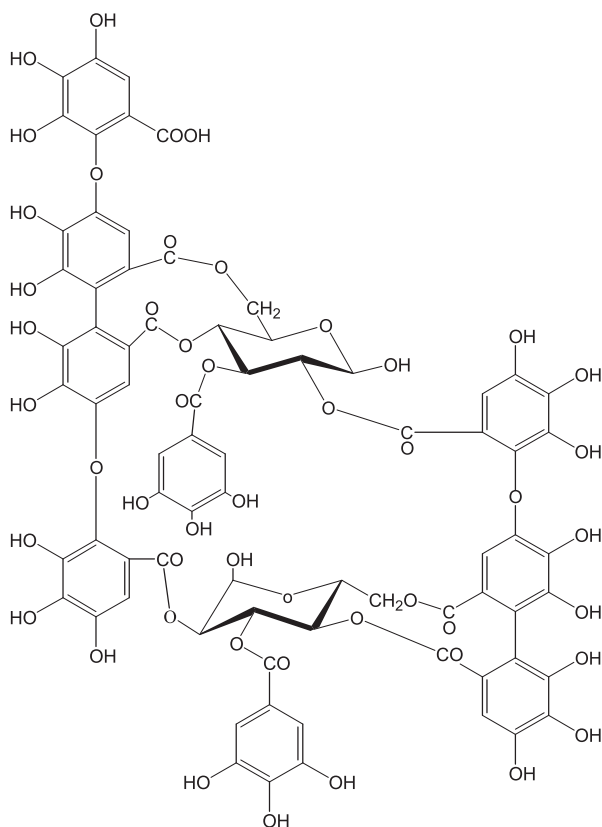


Fig. 1. Chemical structure of woodfordin I.

as Bax, to translocate from the cytosol to mitochondria, leading to the release of cytochrome *c* into cytosol (Liu et al., 1996). Cytochrome *c* then binds to the apoptotic protease activation factor 1 (Apaf-1) and forms a heptamer complex called the apoptosome (Acehan et al., 2002). Apoptosome recruits and activates caspase-9, which in turn activates the downstream executioner caspases, such as caspase-3, 6, and 7 (Li et al., 1997). The second apoptotic pathway is triggered by death-receptor superfamily members through the activation of caspase-8, which can directly activate downstream caspases, leading to cellular degradation. The death-receptor and mitochondrial pathways converge at the level of caspase-3 activation. It is feasible to differentiate them by evaluating the activities of caspase-8 and caspase-9.

Mitochondria play the pivotal roles in integrating and directing death signal towards caspase cascade. They are responsible for a variety of key events in apoptotic process, such as changes in electron transport, loss of mitochondrial transmembrane potential (MMP,  $\Delta\Psi_m$ ) (Marchetti et al., 1996), failure of  $Ca^{2+}$  control, generation of reactive oxygen species (ROS) (Simizu et al., 1998), and release of caspase activators. In particular, Bcl-2 family members, including pro- (such as Bax) or anti-apoptotic (such as Bcl-2 and Bcl-x<sub>L</sub>) proteins, have been proposed to be critical in the regulation of mitochondrial homeostasis (Rosse et al., 1998). The different signals that converge on mitochondria to trigger or inhibit these events and their downstream effects

delineate the major apoptotic pathways. Since a common feature of many drugs and toxicants is an early loss of MMP that appears to be linked to the induction of the mitochondrial permeability transition (MPT) (Kroemer et al., 1998; Zamzami et al., 1995), the mitochondrial dysfunction and subsequent apoptotic cell death may be an underlying effector mechanism for these cytotoxic agents. It is noticeable that drug resistance and tumorigenesis are mainly due to the defects of apoptotic machinery. Understanding the molecular events that contribute to drug-induced apoptosis will enable a more rational approach to cancer chemotherapy.

We investigated woodfordin I for its effect on apoptotic cell death using human chronic myelogenous leukemia (CML) K562 cells. CML is a malignancy of pluripotent hematopoietic cells with the presence of the Philadelphia t(9;22) chromosome (Sawyers et al., 1991). The reciprocal

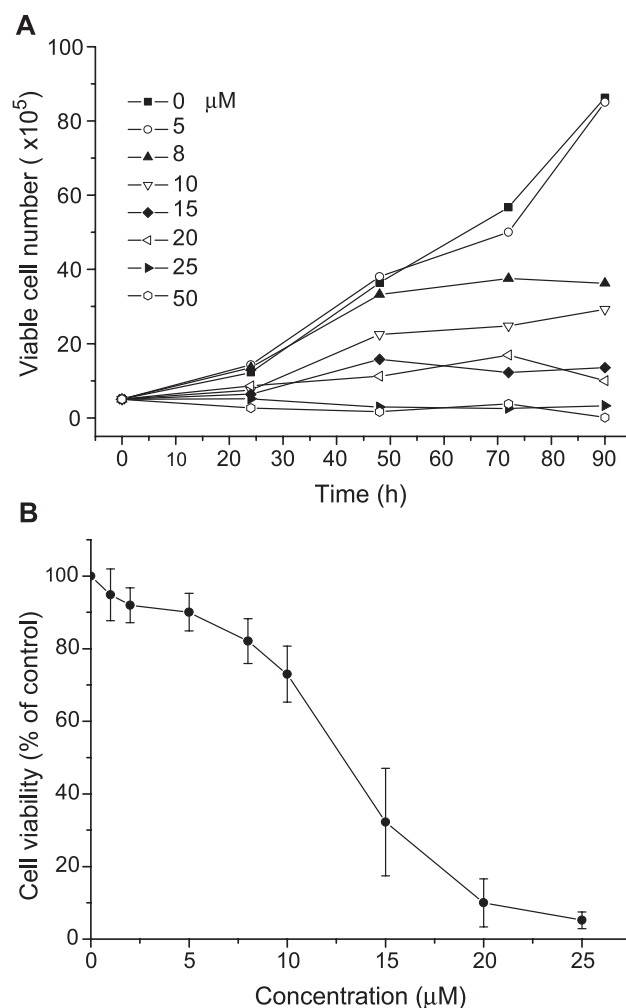


Fig. 2. Effects of woodfordin I on the proliferation and viability of K562 cells. (A) K562 cells were incubated with different concentrations of woodfordin I for the indicated times. The number of viable cells was measured in triplicate by trypan blue exclusion assay. Each point represents the mean of the results obtained from three independent experiments. (B) K562 cells were treated with woodfordin I at the indicated concentrations for 48 h and the viability was determined by MTT assay. Each point is the mean of three replicates; scale bars represent the standard deviation.

translocation generates a chimeric Bcr-Abl protein with dysregulated tyrosine kinase activity, which is the principal driving force for oncogenesis (Lugo et al., 1990). Recent studies suggest that Bcr-Abl appears to act as an apoptotic suppressor through blocking mitochondrial release of cytochrome *c* and activation of caspase-3 (Amarante-Mendes et al., 1998).

The effects of tannins are often pictured as beneficial for cell survival, such as preventive against oxidative insults and anticarcinogenic. However, their actions are complex and often seemingly antagonistic or paradoxical. For example, although some tannins are described as antioxidant agents

for protecting against cytotoxic insults to cells, others have been reported to be prooxidants and apoptotic. To gain insight into the molecular mechanisms of macrocyclic ellagitannins, we performed the present study to estimate the antiproliferative and pro-apoptotic effects of woodfordin I on K562 cells. The biochemical events relevant to mitochondria were studied time dependently, including the dissipation of MMP, alteration of  $\text{Ca}^{2+}$  homeostasis, ROS generation, and cytochrome *c* release. The contributions of Bcl-2 family members and Bcr-Abl signaling were also under investigation. It was demonstrated that mitochondrial dysfunction was an important early step in the regulation of apoptotic process.

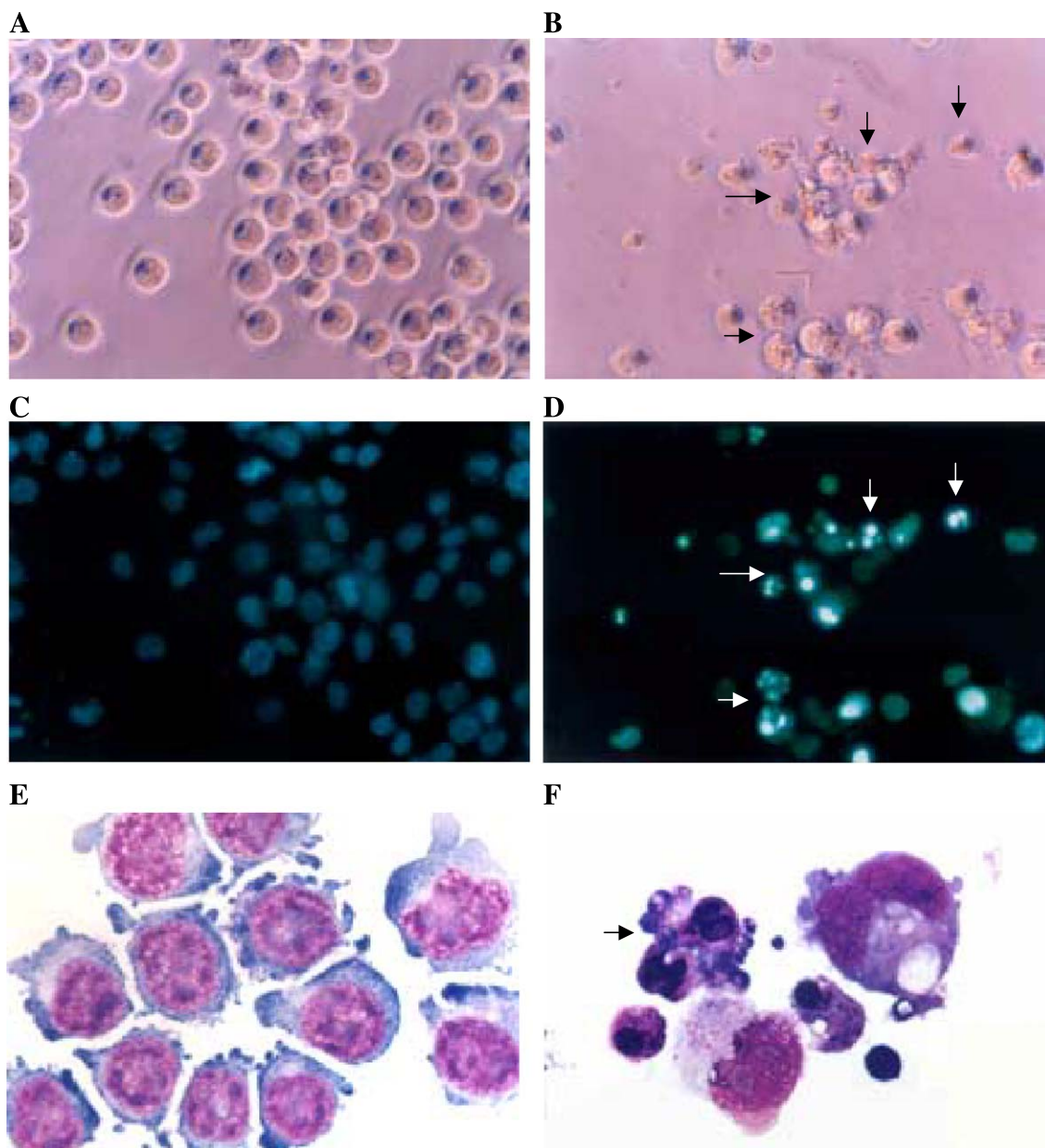


Fig. 3. Morphological changes of K562 cells after exposure to woodfordin I (15  $\mu\text{M}$ ) for 48 h. (A and B) Phase-contrast microscopic view; (C and D) fluorescence microscopic view of the same visual field of (A) and (B); (A and C) untreated cells; (B and D) cells treated with woodfordin I. The condensed chromosomes are seen as spots in the nucleus by DAPI staining; apoptotic cells are shown with arrowheads, magnification  $\times 400$ . (E and F) Wright–Giemsa staining of untreated and woodfordin I-treated cells ( $\blacktriangleright$  the cell with distinct apoptotic bodies), magnification  $\times 1000$ .

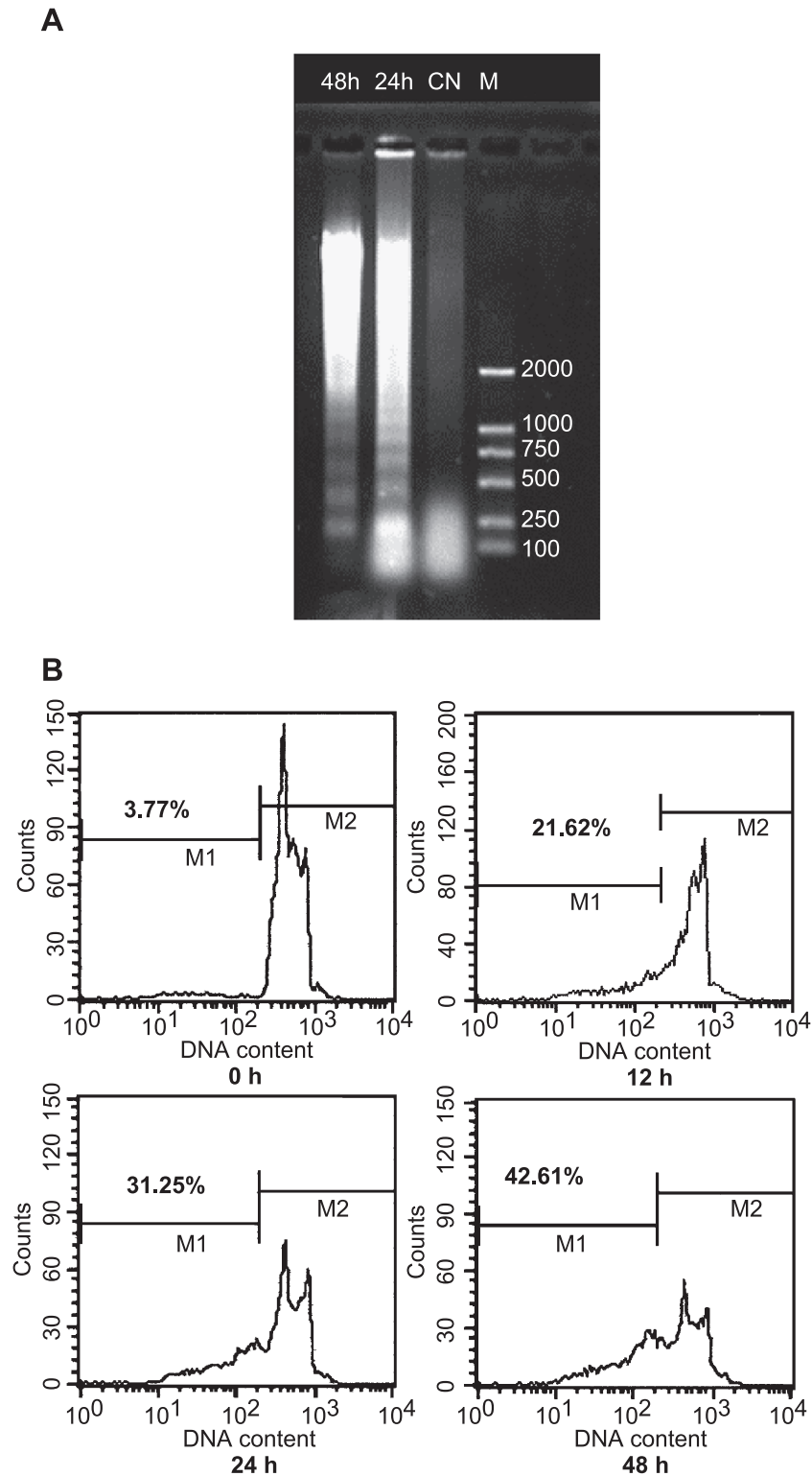


Fig. 4. Apoptosis of K562 cells induced by woodfordin I. K562 cells were treated with or without woodfordin I (15  $\mu$ M) for indicated times. (A) Agarose gel analysis of internucleosomal DNA fragmentation ladder (M, marker; CN, control). (B) Determination of sub-G1 cells by flow cytometric analysis. M1 indicates the apoptotic peak representing the cells with a sub-diploid DNA content. Cell debris was excluded from the analysis by conventional gating of forward scatter versus side scatter dot plots.

When K562 cells were exposed to low ( $\mu\text{M}$ ) concentrations of woodfordin I, a rapid decline in MMP was observed at approximately 20 min, implicating the fast dysfunction of mitochondria. Understanding the underlying mechanisms of woodfordin I-induced cytotoxicity and apoptosis will lead to new perspectives in toxicology and pharmacology research.

## Materials and methods

**Cell culture.** Human CML cell line K562 was kindly provided by Dr. Li-Sheng Wang (Academy of Military Medical Sciences, Beijing). It was cultured in the RPMI 1640 medium (GIBCO BRL, Life Technologies, Invitrogen Corporation, California), with 10% fetal bovine serum (FBS) (Hyclone Laboratories Inc., Utah), 100 IU/ml penicillin, and 100  $\mu\text{g}/\text{ml}$  streptomycin in humidified air at 37  $^{\circ}\text{C}$  with 5%  $\text{CO}_2$ .

**Isolation and structure determination of woodfordin I.** Woodfordin I was isolated from *C. angustifolium* (L.) Scop according to the literature (Yoshida et al., 1992). The

air-dried whole plant (about 1 kg) was chopped into small pieces and extracted with 70% aqueous acetone at room temperature. The combined extracts were concentrated and the resulting precipitates were removed by filtration. The filtrate was subjected to Diaion HP-20 (Tsk) column chromatography, with a stepwise gradient of methanol (MeOH) in  $\text{H}_2\text{O}$ . The fraction eluting at 40% MeOH was rechromatographed over Toyopearl HW-40 and MCI-gel CHP 20P columns with  $\text{H}_2\text{O}$  containing increasing proportion of MeOH to yield a compound as a brown amorphous powder (230 mg). It exhibited the  $(\text{M} + \text{Na})^+$  ion peak at  $m/z$  1759 in FAB-MS. The structure was identified as woodfordin I by comparison of MS and NMR data with those in the previous report (Yoshida et al., 1992). Its purity was more than 95% based on reversed-phase HPLC analysis. Full details for the process of the isolation and characterization are available on request.

$^1\text{H}$  NMR spectra were measured in  $\text{Me}_2\text{CO}-d_6$  at a Bruker 400 MHz NMR spectrometer, with TMS as an internal standard. Chemical shifts are given in ppm.  $^1\text{H}$  NMR (400 MHz,  $\text{Me}_2\text{CO}-d_6$ ): 7.19, 6.94 (each 2H, s, galloyl), 7.17, 7.04, 6.97, 6.68, 6.52, 6.42, 6.28 (each 1H, valoneoyl and

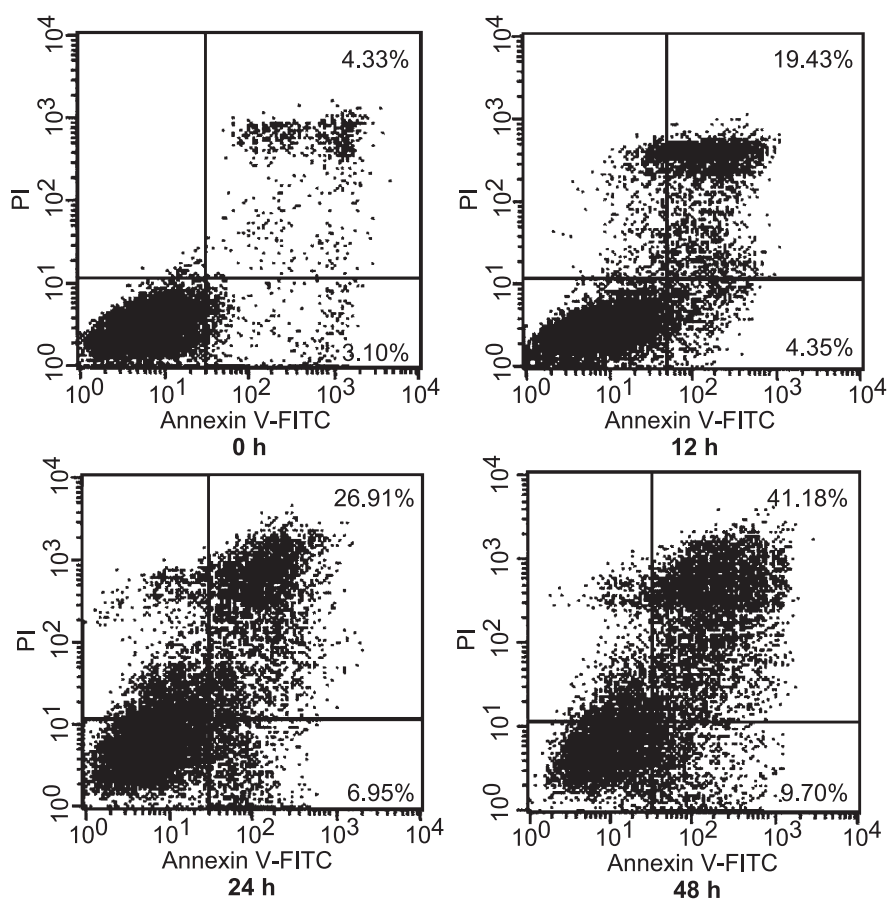


Fig. 5. Flow cytometric analysis of phosphatidylserine externalization (annexin V binding) and cell membrane integrity (PI staining) in K562 cells undergoing apoptosis. K562 cells were treated with woodfordin I (15  $\mu\text{M}$ ) for 0, 12, 24, and 48 h. The dual parametric dot plots combining annexin V-FITC and PI fluorescence show the viable cell population in the lower left quadrant (annexin V<sup>-</sup> PI<sup>-</sup>), the early apoptotic cells in the lower right quadrant (annexin V<sup>+</sup> PI<sup>-</sup>), and the late apoptotic cells in the upper right quadrant (annexin V<sup>+</sup> PI<sup>+</sup>).

woodfordinoyl H). Glucose-I: 6.15 (1H, d,  $J = 2.8$  Hz, H-1), 5.99 (1H, br, H-2), 5.96 (1H, br, H-3), 5.50 (1H, br, H-4), 4.55 (1H, m, H-5), 5.22 (1H, dd,  $J = 6.0, 13.0$  Hz, H-6), 3.62 (1H, dd,  $J = 6.0, 13.0$  Hz, H-6'). Glucose-II: 4.57 (1H, br, H-1), 5.15 (1H, dd,  $J = 8.0, 11.0$  Hz, H-2), 5.37 (1H, t,  $J = 10.0$  Hz, H-3), 4.80 (1H, br, H-4), 4.15 (1H, dd,  $J = 6.0, 10.0$  Hz, H-5), 4.92 (1H, dd,  $J = 6.0, 13.0$  Hz, H-6), 3.75 (1H, dd,  $J = 6.0, 13.0$  Hz, H-6').

**Materials.** Woodfordin I was dissolved in 0.9% NaCl solution (5 mM) and stored at  $-20^{\circ}\text{C}$ . 4',6-Diamidin-2'-phenylindol-dihydrochlorid (DAPI) was purchased from Roche Diagnostics GmbH (Mannheim, Germany). Wright–Giemsa stain (modified), propidium iodide (PI), 3-(4,5-dimethyl-thiazol-2-yl)-2,5-diphenyl-tetrazolium bromide (MTT), saponin, etoposide, and mouse anti- $\beta$ -actin monoclonal antibody (clone AC-74) were bought from Sigma Co. (Missouri). 2',7'-Dichlorodihydrofluorescein diacetate (DCFH-DA), 3',3'-dihexyloxacabocyanine (DiOC<sub>6</sub>(3)) and Fluo-3 were purchased from Fluka Chemie GmbH (Sigma-Aldrich, Steinheim, Switzerland). Mouse anti-cytochrome *c* monoclonal antibody (clone 4CYTC-21) was purchased from R&D Systems, Inc. (NE). Rabbit anti-Bax polyclonal antibody (clone N-20), mouse anti-Bcl-x<sub>L</sub> monoclonal antibody (clone H-5), mouse anti-c-Abl monoclonal antibody (clone 24-11), rabbit anti-caspase-3 polyclonal antibody (clone H-277), and mouse anti-p-Tyr monoclonal antibody (clone pY99) were bought from Santa Cruz Biotechnology Inc. (CA).

**Cell viability.** K562 cells were suspended at a final concentration of  $5 \times 10^4$  cells/ml and seeded in 96-well microtiter plates. Increasing concentrations (1–50  $\mu\text{M}$ ) of woodfordin I were added to each well in triplicate. When incubated for the indicated times, the viable cells were counted by the trypan blue exclusion method. The inhibitory effects were also determined by MTT assay. After exposure to woodfordin I, cells were incubated with MTT (0.5 mg/ml) for 4 h. The formazan precipitate was dissolved in 200- $\mu\text{l}$  dimethyl sulfoxide, and the absorbance at 550 nm was detected with a Benchmark microplate reader (Bio-Rad, California).

**Cytomorphology.** The cells were directly observed under inverted phase-contrast microscopy. Their nuclei in the same visual field were stained with DAPI (10  $\mu\text{g}/\text{ml}$ ) and recorded by fluorescence microscopy (Leica DMIRB and MPS60, Leica Microsystems Wetzlar GmbH, Germany). Meanwhile, cells were centrifuged onto slides by a cytospin (700 rpm, 5 min), stained with Wright–Giemsa stain, and determined by microscopic examination (Leica DMLB).

**DNA fragmentation analysis.** The untreated and woodfordin I-treated cells were harvested and lysed in 100- $\mu\text{l}$  buffer (10 mM Tris-HCl, pH 7.4, 10 mM EDTA, pH 8.0, 0.5% Triton X-100). The supernatant was acquired

through centrifugation at  $14000 \times g$  for 10 min and then incubated with RNase A (200  $\mu\text{g}/\text{ml}$ ) at  $37^{\circ}\text{C}$  for 60 min. Proteins were removed by incubation with Proteinase K (200

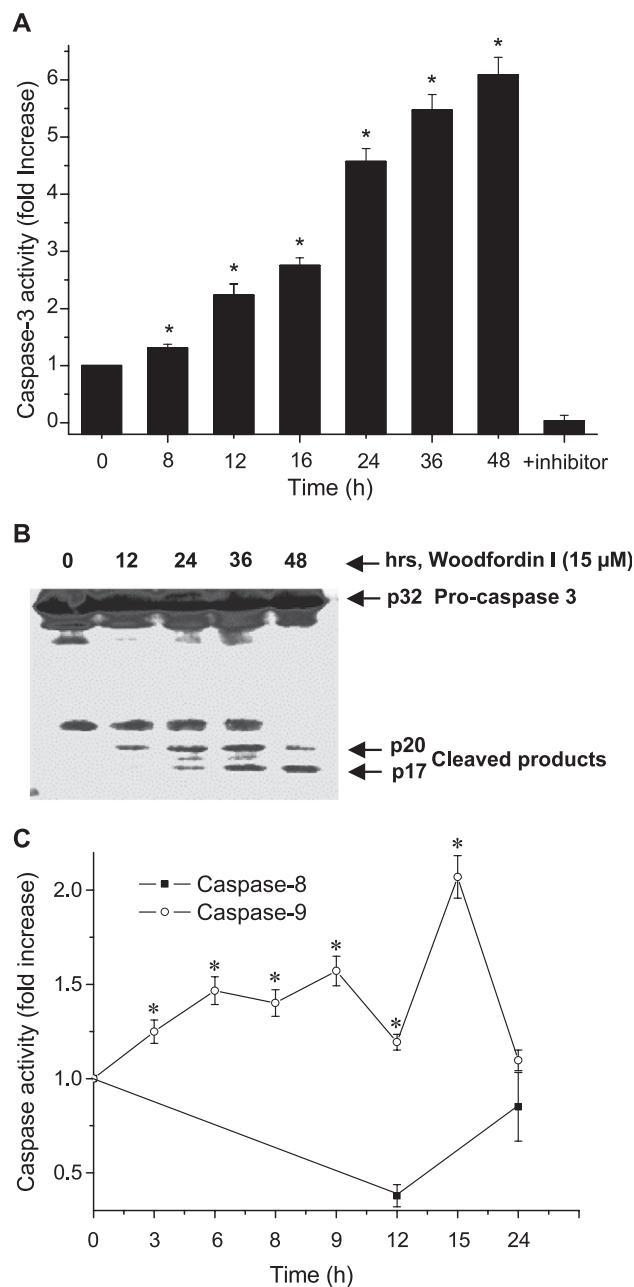


Fig. 6. Activation of caspase-3 and 9, but not caspase-8, during woodfordin I-induced apoptosis. K562 cells were treated with 15  $\mu\text{M}$  woodfordin I for the indicated times. Kinetics of the enzymatic activity of caspase-3 (A), caspase-8 and 9 (C). Data are the mean of three independent experiments and shown as the fold increases in relative fluorescence density. Values are expressed as mean  $\pm$  SD of three independent experiments,  $n = 3$ . \*Significant difference compared with control group (time 0),  $P < 0.05$ . To confirm the results, DEVD-CHO, a caspase-3-specific inhibitor, was added to the induced samples before the addition of the substrate. Whole cell lysates were also analyzed by Western blot assay (B), demonstrating the zymogen procaspase-3 and its activated cleaved fragments (Mr,  $\sim 20$  and  $\sim 17$  kDa).

$\mu\text{g/ml}$ ) at  $50\text{ }^{\circ}\text{C}$  for 30 min. The lysate was added with  $20\text{-}\mu\text{l}$   $5\text{ M NaCl}$  and  $120\text{-}\mu\text{l}$  isopropanol. After it was deposited at  $-20\text{ }^{\circ}\text{C}$  for 12 h, the precipitated DNA pellet was

dissolved in Tris–acetate–EDTA buffer, electrophoresed in a 1.5% agarose gel, stained with ethidium bromide, and photographed under UV illumination.

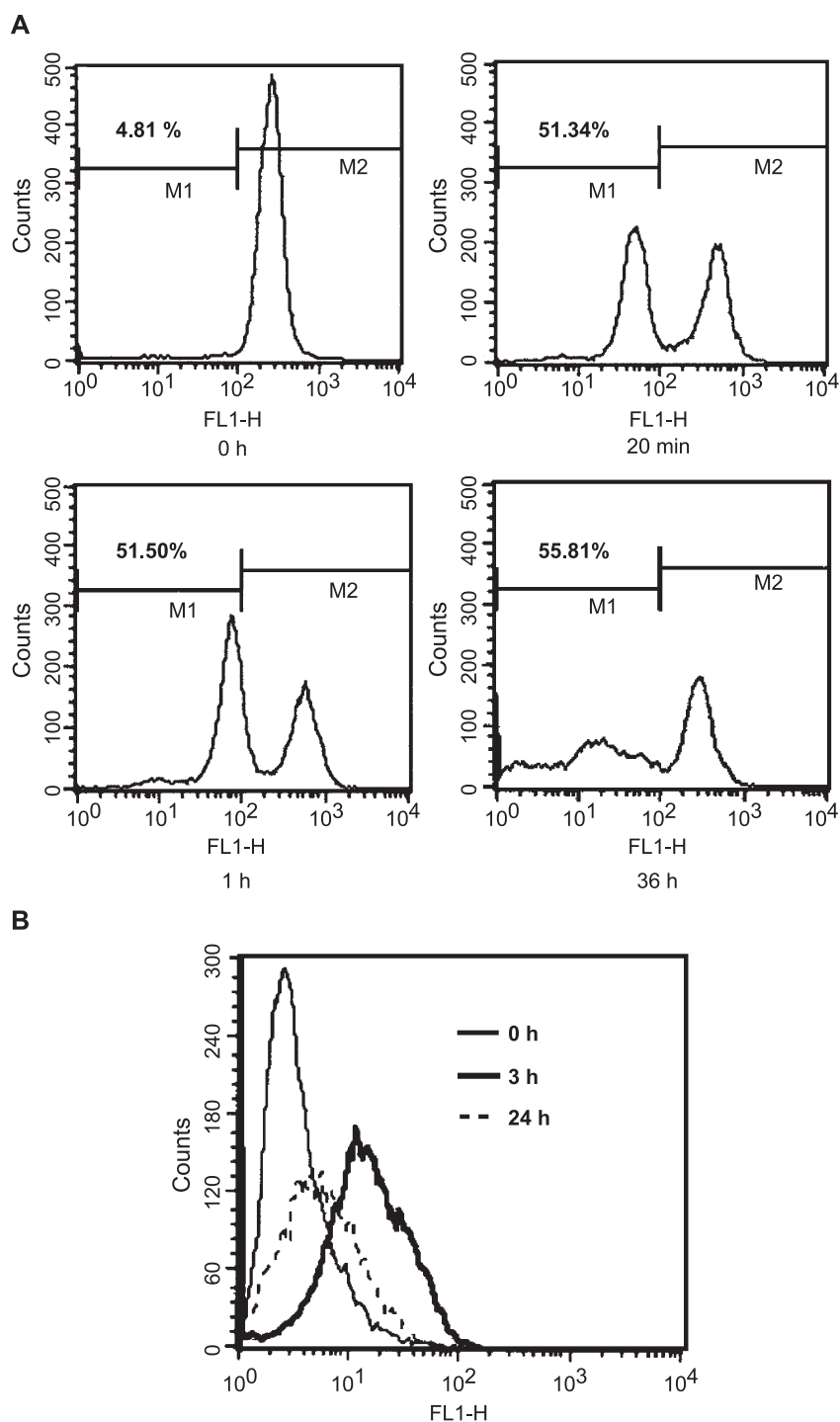


Fig. 7. MMP ( $\Delta\Psi_m$ ) reduction, ROS generation, and cytochrome *c* release from mitochondria into the cytosol during woodfordin I-induced apoptosis. K562 cells were treated with  $15\text{ }\mu\text{M}$  woodfordin I for the indicated times. (A) The loss of MMP (DiOC<sub>6</sub>(3) uptake) was analyzed by flow cytometry and the percentage of M1 reflects the reduction of  $\Delta\Psi_m$ . (B) Flow cytometry analysis of ROS generation (staining by DCFH-DA). (C) Time course analysis for the decline of MMP and generation of ROS in the apoptotic process (MMP decrease: the percentage of the cells that have lower DiOC<sub>6</sub>(3) fluorescence; ROS increase: the percentage of the cells that have higher DCFH-DA fluorescence). (D) Following treatment of K562 cells with  $15\text{ }\mu\text{M}$  woodfordin I and  $100\text{ }\mu\text{M}$  etoposide for 9 h, the cytosol fractions were obtained and analyzed with Western blot analysis. The epipodophyllotoxin etoposide, which is commonly used for the treatment of human tumors, was employed as the positive control. Results are representative of two independent experiments.

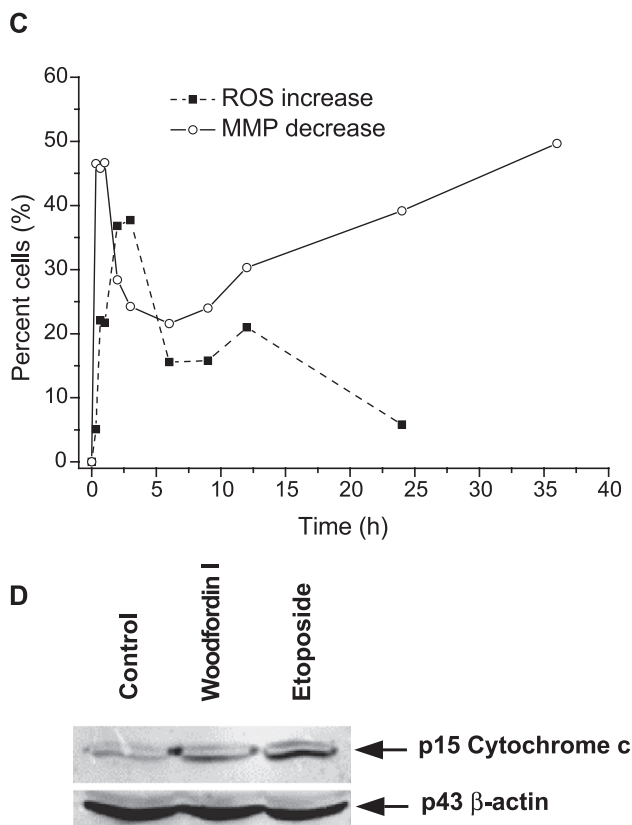


Fig. 7 (continued).

**Flow cytometric analysis of apoptosis.** Cells were fixed by 70% ethanol at  $-20^{\circ}\text{C}$  for at least 12 h. After two washes with phosphate-buffered solution (PBS), the cells were incubated in RNase A/PBS (100  $\mu\text{g}/\text{ml}$ ) at  $37^{\circ}\text{C}$  for 30 min. Intracellular DNA was labeled with PI (100  $\mu\text{g}/\text{ml}$ ) and analyzed with a FACSCalibur fluorescence-activated cell sorter (FACS) using CELLQuest software (Becton Dickinson, New Jersey). We also used the ApoAlert Annexin V-FITC apoptosis detection kit (BD Biosciences Clontech, California) to identify the translocation of phosphatidylserine. Cells were treated and determined with FACS according to the manufacturer's instructions. At least 10000 events were analyzed for each sample.

**Measurement of mitochondrial membrane potential.** Mitochondrial energization was determined by the retention of the dye DiOC<sub>6</sub>(3). About one million cells were harvested and washed twice with PBS. After incubation with 50 nM DiOC<sub>6</sub>(3) at  $37^{\circ}\text{C}$  for 30 min, the cells were washed again and analyzed with FACS.

**Assessment of caspase activity.** ApoAlert caspase fluorescent and colorimetric assays (BD Biosciences Clontech, California) were used to determine the enzyme activity of caspases-3, 8, and 9. After being incubated with woodfordin I (15  $\mu\text{M}$ ) for various time intervals, cells were collected and lysed in ice-cold buffer. Homogenate was

clarified by centrifugation at  $12000 \times g$  for 10 min at  $4^{\circ}\text{C}$ . Caspase activities in the supernatant were determined by cleavage of the specific chromophore-conjugated substrates. The substrate peptides of caspase-3, 8, and 9 (DEVD, IETD, and LEHD) were conjugated to 7-amino-4-trifluoromethyl coumarin (AFC), *p*-nitroaniline (*p*-NA), and 7-amino-4-methyl coumarin (AMC), respectively. The release of AFC and AMC (for caspase-3 and 9) was measured by quantifying fluorescent intensity in a fluorescence spectrophotometer (Hitachi F-2500, Japan). Caspase-8 activity was determined by absorbance of *p*-NA at 405 nm in a microplate reader.

**Measurement of intracellular ROS generation.** Intracellular ROS production was measured by using a fluorescent dye, DCFH-DA, which can be converted to DCFH by esterases when the cell takes it up. DCFH is reactive with ROS to give a new highly fluorescent compound, dichlorofluorescein, which can be analyzed with FACS. The treated cells were incubated with DCFH-DA (10  $\mu\text{M}$ ) at  $37^{\circ}\text{C}$  for 1 h, and then measured with the FACS.

**Analysis of intracellular  $\text{Ca}^{2+}$  concentration.** The changes of intracellular  $\text{Ca}^{2+}$  concentration were determined by a fluorescent dye, Fluo-3. Cells were washed twice with RPMI 1640 medium and incubated with 5  $\mu\text{M}$  Fluo-3 at  $37^{\circ}\text{C}$  for 30 min. Then, the cells were washed and analyzed with FACS.

**Immunofluorescence analysis.** Cells were harvested and washed with PBS containing 3% FBS twice. After being fixed in 4% paraformaldehyde at  $4^{\circ}\text{C}$  for 15 min, cells were washed and resuspended in PBS buffer containing 0.2% saponin and 5% FBS. The FITC-conjugated mouse anti-human Bcl-2 monoclonal antibody and IgG<sub>1</sub> isotype control (BD Biosciences PharMingen, CA) were added. After incubation at  $4^{\circ}\text{C}$  for 30 min, cells were washed and analyzed with FACS. For Bax protein, the fixed and permeabilized cells were incubated with either rabbit anti-Bax polyclonal antibody or IgG<sub>1</sub> isotype at  $4^{\circ}\text{C}$  for 30 min. After being washed with PBS, cells were incubated with FITC-conjugated goat anti-rabbit IgG<sub>1</sub> antibody for another 30 min and were analyzed with FACS.

**Western blot.** Cells were harvested and washed with PBS. The lysates were achieved with lysis buffer (150 mM NaCl, 10 mM Tris, pH 7.4, 5 mM EDTA, pH 8.0, 1% Triton X-100, 1 mM PMSF, 20  $\mu\text{g}/\text{ml}$  aprotinin, 50  $\mu\text{g}/\text{ml}$  leupeptin, 1 mM benzaidine, 1  $\mu\text{g}/\text{ml}$  pepstatin), followed with centrifugation ( $10000 \times g$ , 20 min). Total protein concentration in the supernatant was determined with Bicinchoninic Acid assay (Beyotime biotechnology, China). To analyze cytochrome *c* in the cytosol, the washed cells were resuspended in homogenization buffer (20 mM HEPES, pH 7.5, 1 mM EGTA, 1 mM EDTA, 10 mM KCl, 1.5 mM  $\text{MgCl}_2$ , 1 mM DTT, 0.1 mM PMSF, 2  $\mu\text{g}/\text{ml}$  leupeptin, 2  $\mu\text{g}/\text{ml}$  pepstatin,

2 µg/ml aprotinin) and broken by 40 strokes with a pestle in a glass homogenizer on ice. Nuclei were removed by centrifugation at  $800 \times g$  for 10 min. After being centrifuged again at  $10000 \times g$  for 15 min, the supernatant was

collected as a cytosolic fraction. Proteins were normalized to 50 µg/lane, resolved on 7.5% (Bcr-Abl), 10% (p-Tyr), 12.5% (Bcl-x<sub>L</sub> and Bax), and 15% (caspase-3 and cytochrome *c*) polyacrylamide gels, and subsequently blotted

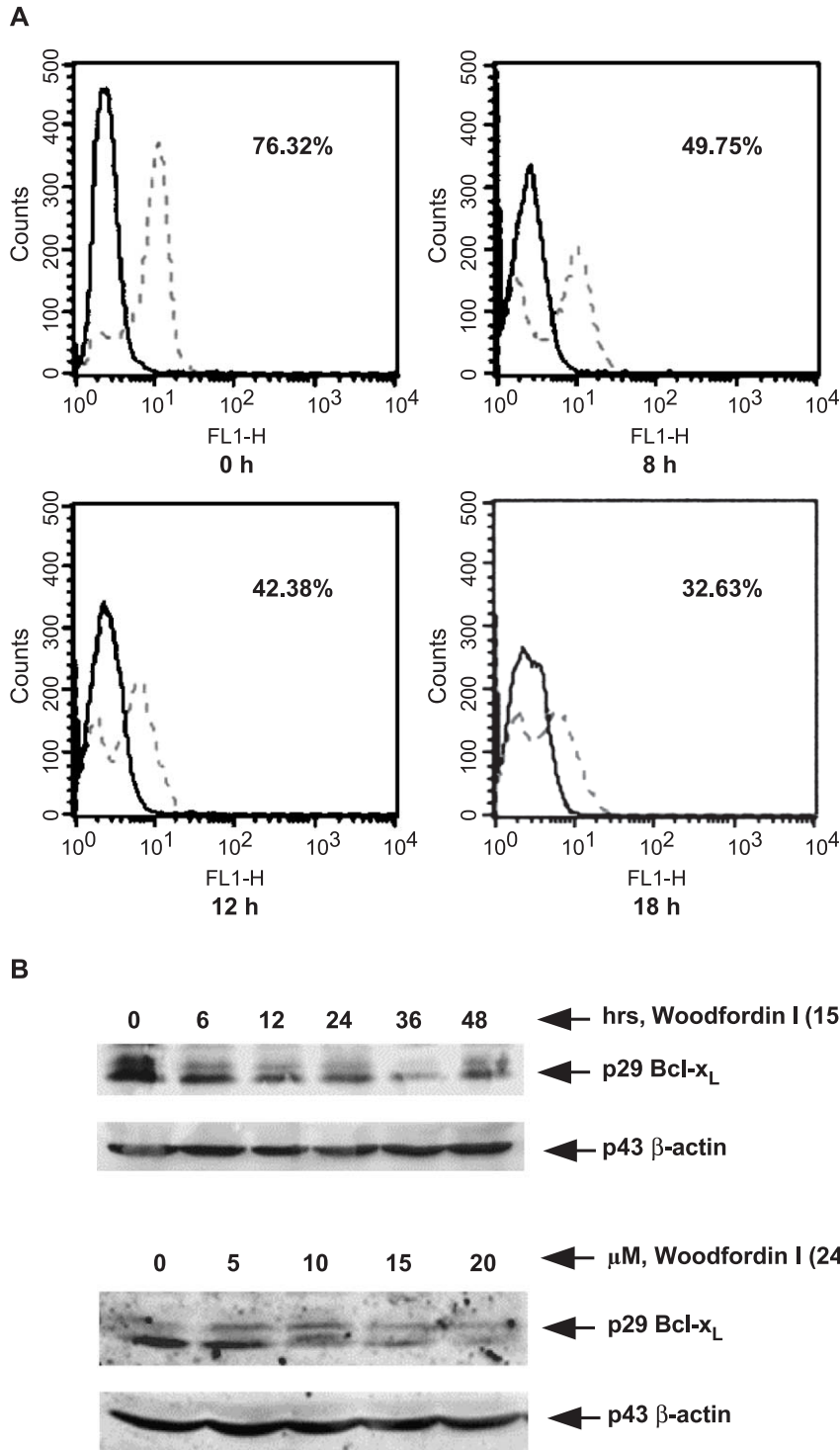


Fig. 8. Woodfordin I decreases the levels of Bcl-2 and Bcl-x<sub>L</sub>. (A) Immunofluorescence analysis of Bcl-2 expression. The solid lines indicate mouse IgG<sub>1K</sub> used as isotype control, while the dotted lines represent woodfordin I-treated K562 cells. At least 10000 events were counted. Data shown are representative of three separate experiments. (B) Western blot analysis of Bcl-x<sub>L</sub> levels in untreated and woodfordin I-treated K562 cells. β-Actin was used as an internal control to identify equal amounts of proteins loaded in each lane.

onto PVDF sheets. After blocking with TTBS (100 mM Tris-HCl, pH 7.5, 0.9% NaCl, 0.1% Tween 20) containing 5% (w/v) skim milk, the sheets were incubated with antibodies for 1 h at room temperature. Then, the membranes were washed with TTBS and detected with an ECF Western blotting kit. The densities of sample bands were determined with a fluorescence scanner (Storm 860) and analyzed with the ImageQuant software (Amersham Biosciences UK Limited, England).

**Statistical analysis.** One-way analysis of variance (ANOVA) was performed to determine the significance between groups. A *P* value of less than 0.05 ( $P < 0.05$ ) was considered as statistically significant.

## Results

### Woodfordin I suppresses the growth of K562 cells

The effects of woodfordin I on the growth and survival of human CML K562 cells were first assessed. Cell proliferation was evaluated daily based on the ability of the cells to exclude trypan blue. At concentrations from 5 to 50  $\mu$ M, woodfordin I induced a marked time- and dose-dependent diminution of cell viability as early as 24 h (Fig. 2A). The decrease of viable cell number in the presence of woodfordin I suggested that the proliferation potential of the cells was impaired. The cell viability was also determined by MTT assay, and the  $IC_{50}$  (median growth inhibitory concentration value) was as low as about 10  $\mu$ M (Fig. 2B).

### Woodfordin I induces apoptosis in K562 cells

Fig. 3 shows the representative morphological changes of K562 cells exposed to woodfordin I (15  $\mu$ M) for 48 h. Under control conditions, K562 cells appeared normal and the nuclei were round and homogeneous (Figs. 3A, C, E). After being treated with woodfordin I, the cells exhibited the characteristic features of apoptosis, such as plasma membrane blebbing and cell shrinkage (Fig. 3B). Nuclear condensation and fragmentation were assessed by DAPI staining (Fig. 3D). Wright-Giemsa stain distinctly showed the formation of apoptotic bodies (Fig. 3F).

In accordance with morphological changes, woodfordin I induced the typical formation of DNA fragments as ladders of ~200 bp on agarose gels in a time-dependent manner, which is the biochemical hallmark of apoptosis (Fig. 4A). The DNA content-frequency histograms showed a distinct sub-G1 peak, which has been suggested to be the apoptotic DNA (Fig. 4B). Furthermore, we performed annexin V/PI binding assay to detect the redistribution of phosphatidylserine, which is a hallmark for early apoptotic cells (van Engeland et al., 1998). In untreated K562 cells, 3.1% of cells were annexin V-positive/PI-negative, whereas 4.3% of

cells were annexin V/PI double positive. The treatment of 15  $\mu$ M woodfordin I for 48 h increased the annexin V-positive/PI-negative cells to 9.7% and the double positive cells to 41.18% (Fig. 5).

### Woodfordin I induces the activation of caspase-3 and 9, but not caspase-8 in the apoptotic process

We then asked whether caspases were activated in the cell death response induced by woodfordin I. As shown in Fig. 6A, woodfordin I (15  $\mu$ M) induced a dramatic increase of caspase-3 activity in K562 cells in a time-dependent manner. It was approximately sixfold compared to the control group when cells were treated for 48 h. Western blot analysis also demonstrated the same results (Fig. 6B). Caspase-3 was present in control cells primarily as 32 kDa zymogen. Woodfordin I treatment induced a time-dependent activating process accompanied by the formation of two major cleaved products, 20 and 17 kDa fragments (Nicholson et al., 1995). It is noteworthy that the relative abundance of these fragments increased during apoptosis. Caspase-9 was activated as early as 3 h after woodfordin I treatment, indicating its activation was an upstream event before caspase-3 processing. In contrast, negligible caspase-8 activity was observed at 12 and 24 h, suggesting no involvement of caspase-8 in the apoptotic process (Fig. 6C).

### Woodfordin I induces loss of MMP, transient increase of ROS, and release of cytochrome c into cytosol

One of the early events in apoptotic signaling appears to be the alteration of mitochondrial membrane integrity. The

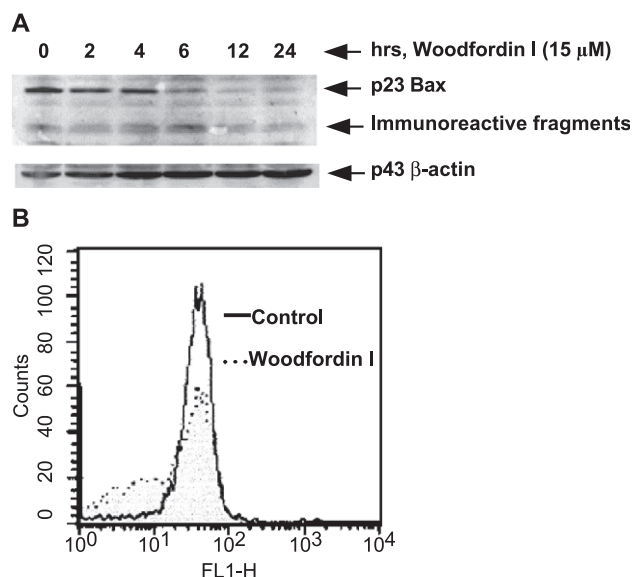


Fig. 9. Woodfordin I downregulates Bax levels. (A) Western Blot analysis shows the decline of Bax levels time dependently when K562 cells were treated with 15  $\mu$ M woodfordin I. (B) Immunofluorescence analysis for Bax was performed. After exposure of cells to 15  $\mu$ M woodfordin I for 12 h, Bax levels decreased distinctly.

effects of woodfordin I on MMP ( $\Delta\Psi_m$ ) of K562 cells were evaluated. As shown in Fig. 7A, the fluorescence intensity of DiOC<sub>6</sub>(3) shifted to the left as early as 20 min, demonstrating the efficiency of woodfordin I in depolarizing mitochondria. Generation of ROS might be a relatively later event, which was determined by DCFH-DA. It increased gradually in the first 3 h, but decreased quickly after that (Figs. 7B, C). Time course analysis confirmed that woodfordin I induced a fast and sustained decline in MMP,

but a transient increase in ROS (Fig. 7C). Cytochrome *c* release into cytosol is an almost universal feature of apoptotic cell death. Fig. 7D shows that a marked increase in the cytosolic cytochrome *c* level was observed following an exposure to 15  $\mu$ M woodfordin I for 9 h with etoposide as the positive control. Taken together, these findings suggest that woodfordin I induced mitochondrial dysfunction, resulting in the release of cytochrome *c* and subsequent activation of caspase cascade, indicating that the

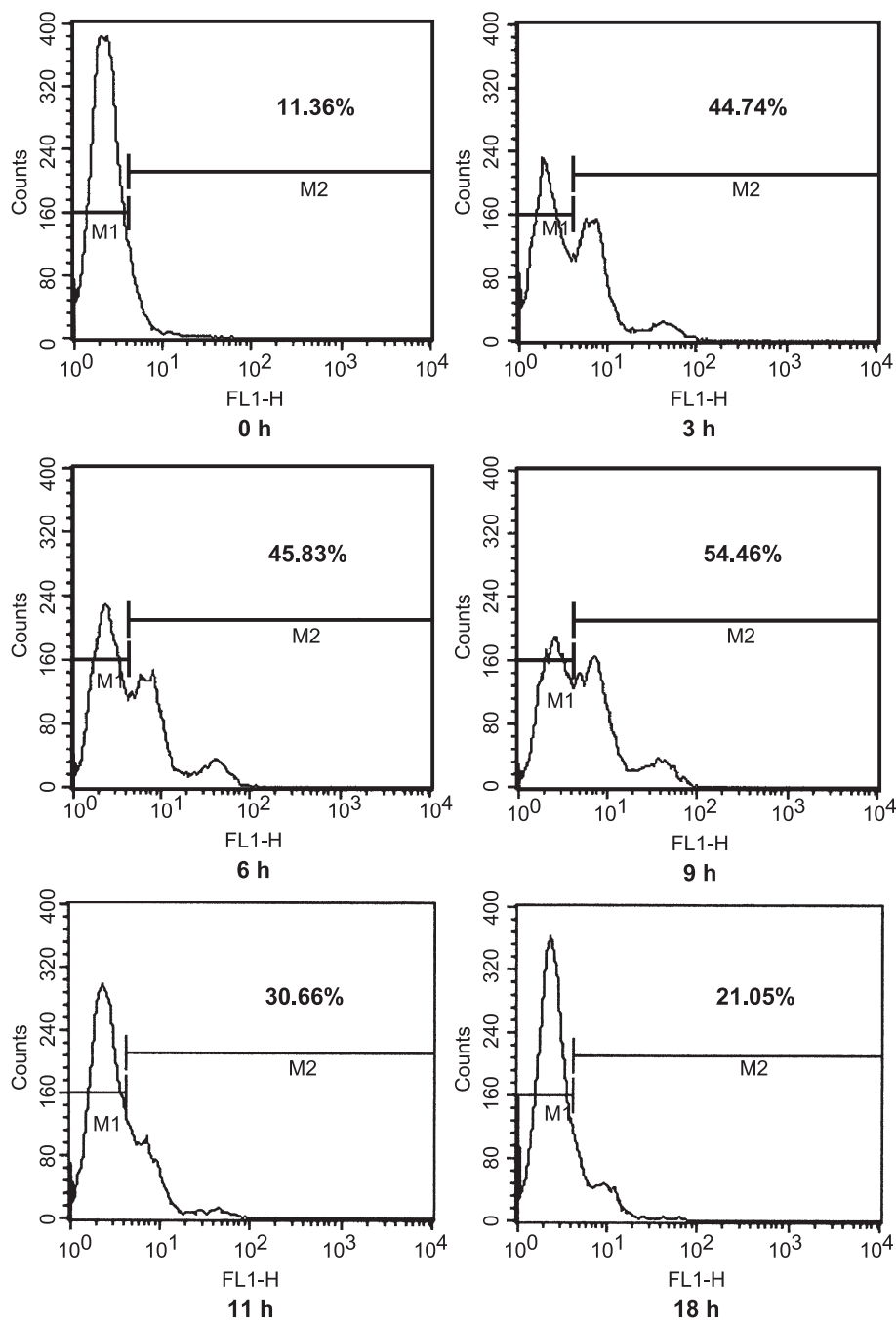


Fig. 10. Time course analysis of the Ca<sup>2+</sup> concentration during apoptotic process. K562 cells were treated with 15  $\mu$ M woodfordin I for the indicated times. The intracellular Ca<sup>2+</sup> concentration was determined by the fluorescence of Fluo-3 with FACS.

intrinsic mitochondria-dependent pathway was involved in the apoptotic process.

*The levels of anti-apoptotic Bcl-2, Bcl-x<sub>L</sub>, and pro-apoptotic Bax are downregulated by woodfordin I*

As shown in Fig. 8A, the Bcl-2 level was determined by immunofluorescence analysis, which decreased gradually with time. Another anti-apoptotic protein Bcl-x<sub>L</sub> was also downregulated by woodfordin I in a time- and dose-dependent manner (Fig. 8B). Of special interest is the significant decline of the pro-apoptotic Bax level, when normalized to the intracellular β-actin serving as the control (Fig. 9A). The concomitant appearance of smaller immunoreactive fragments suggests that this may be the result of Bax proteolysis or cleavage. Immunofluorescence analysis of Bax also showed the same results (Fig. 9B).

*Woodfordin I induces the transient elevation of Ca<sup>2+</sup> concentration*

Fig. 10 shows that woodfordin I treatment rapidly enhanced the intracellular Ca<sup>2+</sup> level as early as 3 h. The fluorescence intensity of Fluo-3 reached to a maximum when cells were treated for about 9 h and decreased quickly after that, indicating that the elevation of Ca<sup>2+</sup> concentration is an important initial step for woodfordin I-induced apoptosis.

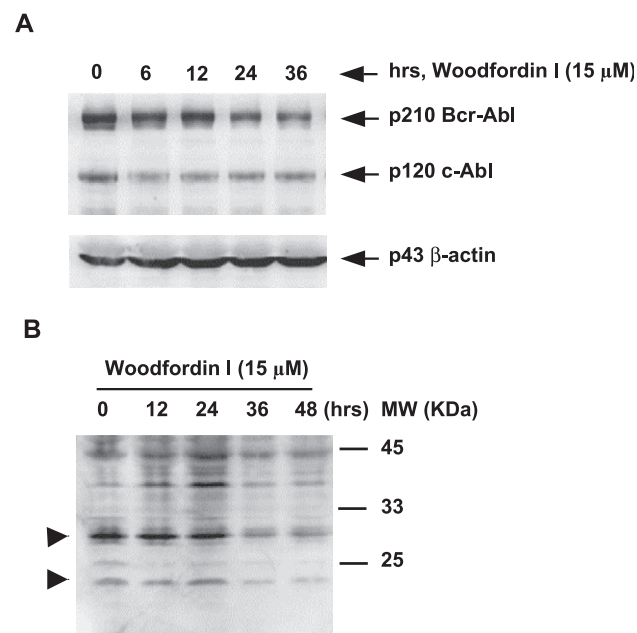


Fig. 11. Western blot analysis of the levels of c-Abl, Bcr-Abl, and tyrosine phosphorylated proteins. K562 cells were treated with 15 μM woodfordin I for the indicated times. Woodfordin I induces downregulation of p120 c-Abl, p210 Bcr-Abl (A), and decreases tyrosine phosphorylation of some polypeptides (▶) in K562 cells (B). β-Actin expression was used as control for equal amounts of proteins loading (A).

*Woodfordin I lowers the levels of Bcr-Abl and inhibits tyrosine phosphorylation in K562 cells*

We determined the effects of woodfordin I on Bcr-Abl signaling. As shown in Fig. 11A, the expression levels of p120 c-Abl and p210 Bcr-Abl were downregulated when K562 cells were treated with woodfordin I (15 μM) for longer intervals. c-Abl and Bcr-Abl began to decrease as early as 6 h. This downregulation was followed by additional changes in the tyrosine phosphorylation of other cellular peptides. Blotting with anti-phosphotyrosine antibodies revealed decreased tyrosine phosphorylation of at least two cellular polypeptides at 24 h, suggesting that inhibition of p210 Bcr-Abl kinase activity was followed by reduction of phosphorylation on downstream signaling transducers (Fig. 11B).

## Discussion

Natural products have been used in traditional and folk medicine for therapeutic purposes. They provide one of the most important sources of promising leads for the development of novel therapeutics. The ellagitannin family of plant polyphenols spans a class of over 500 structurally diverse members. An increasing interest in the role played by these secondary plant metabolites in tannin-rich folk medicine from China has led to the identification of several ellagitannins, which display high levels of chemopreventive and antitumor activities. Macrocyclic ellagitannins, a kind of ellagitannin with distinct structures, have been reported to have remarkable biological and pharmacological activities, such as apoptosis induction, host-mediated antitumor activity, and inhibition of tyrosine kinases (Polya et al., 1995). Their curative role is probably exerted by virtue of three distinctive characteristics, including the complexation with metal ions, radical scavenging activity, and ability to combine with macromolecules such as proteins and polysaccharides (Haslam, 1996). Woodfordin I, an ellagitannin dimer, was employed in this study and its mechanism to induce K562 cell apoptosis was investigated in detail. The results demonstrated that woodfordin I treatment initiated a series of events leading to apoptotic cell death, such as mitochondrial dysfunction, caspase activation, and DNA fragmentation.

Caspases are the central executioners of apoptosis. The initiator caspases (e.g., caspase-8 and 9) respond to various stimuli and subsequently catalyze the activation of more abundant and catalytically robust 'effector' caspases (e.g., caspase-3 and 7) that largely perform the proteolytic cleavage events necessary to mediate the apoptotic phenotype. In this study, caspase-3 was activated when cytochrome *c* was released into cytosol following the collapse of MMP. It was the decisive point during the commitment stage of apoptosis (Fig. 6). The low activity of caspase-8 in K562 cells demonstrated that the death-receptor pathway was not

activated. On the other hand, the processing of caspase-9, as well as the cytosolic accumulation of cytochrome *c*, confirmed that the mitochondria-dependent (intrinsic) pathway contributed to the woodfordin I-induced apoptosis. Since K562 cells lack a functional p53, our data also indicated that p53 is not an obligatory participant in these cells (Lubbert et al., 1988).

Mitochondrial homeostasis plays a pivotal role in regulating apoptosis. Pro-apoptotic signals (i.e., ROS, altered redox status, and increases in  $\text{Ca}^{2+}$  levels) can trigger the mitochondria to release caspase-activating proteins into cytosol, such as cytochrome *c*, AIF, and Smac/DIABLO, subsequently committing the cell to die by Apaf-1-mediated activation of the caspase-9 and caspase-3. We show that woodfordin I induced a fast and sustained collapse of MMP ( $\Delta\Psi_m$ ), which reflected the perturbation of the inner membrane (Fig. 7). It appeared in the cells that still lacked obvious morphological signs of apoptosis. The decline of MMP was temporally correlated with the opening of the permeability transition pore (Zamzami et al., 1996), leading to the release of caspase-activating proteins. Recent studies have shown that this rapid and sustained loss of MMP reflects a block of respiratory function, which is not due to the dispersal of cytochrome *c* (Waterhouse et al., 2001), but due to the cleavage and inactivation of electron transport chain constituents by activated caspases (Ricci et al., 2003). Because mitochondrial dysfunction was prevalent in the early stages of woodfordin I treatment, it should be directly responsible for the apoptotic cell death observed. Moreover, we believe that a threshold of mitochondrial destruction needs to be reached before a cell die.

MMP disruption precedes the major changes in cellular redox potentials (ROS), which is an important determinant in apoptotic signaling transduction (Cadenas and Davies, 2000). ROS is known as an intracellular second messenger at low concentrations and is able to activate transcription factors such as NF- $\kappa$ B and AP-1 (Hockenbery et al., 1993). Its burst in the cytosol, mainly caused by mitochondria disruption, might act as a mediator in apoptotic signaling pathways (Fig. 7). ROS can in turn act on MMP and influence mitochondrial function, mediate the elevation of intracellular  $\text{Ca}^{2+}$ , and lead to the activation of executioner caspases. Furthermore, the transient elevation of ROS in our studies is able to offer a new insight into the effects of tannins because previous studies showed that they can block or delay apoptosis via removal of ROS (Kelso et al., 2001). Although most plant-derived polyphenolic antioxidants including tannins and flavonoids are known to act as antioxidants, the apoptosis-inducing effects of woodfordin I are assumed to its prooxidant action.

Bcl-2 and Bcl-x<sub>L</sub> have been previously shown to exert their inhibitory effects on apoptosis by blocking the release of cytochrome *c* and decline of mitochondrial MMP (Ibrado et al., 1996; Yang et al., 1997). Woodfordin I downregulated their expression levels in the process of K562 cell death, in conjunction with the impairment of their anti-apoptotic roles (Fig. 8). It is unexpected and interesting to find that the level

of pro-apoptotic Bax diminishes as early as 6 h during apoptosis, accompanied by the appearance of smaller immunoreactive fragments (Fig. 9). Bax mainly resides in cytosol and translocates to mitochondria upon receiving an apoptotic signal, where it may initiate homo- or heterodimerization (Wolter et al., 1997), resulting in the mitochondrial dysfunction (Gross et al., 1998). To explain the decrease of Bax immunoreactivity, we introduce a hypothesis that Bax is entirely likely to gain access into the intermembrane space and then be cleaved by calpain, resulting in enhanced cytotoxic activity of the cleavage fragment (Wood and Newcomb, 2000). The cleaved Bax might favorably insert into the inner membrane and form an ion channel, leading to the release of cytochrome *c* (Schlesinger et al., 1997). The immunoreactive amino terminus of Bax may be cleaved so that the antibody cannot detect it, leading to the decrease of the whole protein levels.

Woodfordin I induced a transient elevation of cytoplasmic  $\text{Ca}^{2+}$  concentration before caspase-3 activation, suggesting that the  $\text{Ca}^{2+}$  homeostasis plays an important role in the apoptotic process (Fig. 10). The redistribution of plasma membrane phosphatidylserine has been known to be regulated by the  $\text{Ca}^{2+}$  levels at the membrane, as well as by energy-dependent lipid-transporting enzymes (Hampton et al., 1996).  $\text{Ca}^{2+}$  was also associated with ROS generation (Sakaguchi et al., 1998), NF- $\kappa$ B activation, alterations of mitochondrial function, and the direct activation of proteases (e.g., calpain and  $\text{Ca}^{2+}$ -dependent endonuclease). Two hypotheses have been proposed to explain the involvement of  $\text{Ca}^{2+}$  in the apoptotic process (McConkey and Orrenius, 1997). The first one is that the depletion of intracellular stores (such as endoplasmic reticulum) and possibly the influx of extracellular  $\text{Ca}^{2+}$  promote the increase of cytoplasmic  $\text{Ca}^{2+}$  that acts as a signal for apoptosis, perhaps by activating key catabolic enzymes that make up the effector machinery. The second hypothesis proposed is that it is mainly the emptying of intracellular  $\text{Ca}^{2+}$  stores that trigger apoptosis, perhaps by disrupting the intracellular architecture thus allowing key elements of the effector machinery (such as DNase I) to gain access to their substrates.

c-Abl is a non-receptor tyrosine kinase with both cytoplasmic and nuclear localization. The nuclear version is activated in response to DNA-damaging agents by binding to ataxia-telangiectasia protein (Yuan et al., 1996). The oncogenic activity of Bcr-Abl is due in large part to the induction of the proliferation and prolonged survival of precursor stem cells, which in CML leads to accumulation of granulocytes. Bcr-Abl confers resistance to apoptosis induced by many anticancer drugs (Bedi et al., 1994), which is, in part, mediated by prolonging the G<sub>2</sub>/M checkpoint and allowing DNA repair mechanisms to operate post-genotoxic insult (Bedi et al., 1995). Fig. 4B shows that most of K562 cells were arrested at G<sub>2</sub>/M phase at 12 h. Woodfordin I downregulated Bcr-Abl levels and changed the distribution of cell cycle at 24 h (Figs. 4B and 11A). Bcr-Abl can also phosphorylate a large number of sub-

strates and thereby activate many signal transduction pathways such as Ras-Raf-ERK, JAK-STAT, PI (3) K, and NF- $\kappa$ B. Our results show that woodfordin I lowered the expression levels of p120 c-Abl and p210 Bcr-Abl, indicating the reduction of their tyrosine kinase activity. The decline of the cellular protein tyrosine phosphorylation levels suggested that some presumed downstream targets were suppressed largely (Fig. 11). These observations demonstrate that Bcr-Abl inhibition, which is accompanied by decreased tyrosine phosphorylation of some cellular proteins, participates in the apoptotic signaling transduction pathway.

In conclusion, woodfordin I, a macrocyclic ellagitannin dimer, causes fast mitochondrial dysfunction and induces apoptosis in human CML K562 cells through the intrinsic pathway. Our results demonstrate that it may serve as a novel promising lead compound in cancer chemotherapy, although extended *in vivo* studies are warranted to be performed. In a word, the present study will open interesting perspectives in the research of toxicology and pharmacology for macrocyclic ellagitannins.

## Acknowledgments

This work was supported in part by the grants from the Tsinghua University—Hong Kong Baptist University Joint Institute for Research of Chinese Medicine, and Tsinghua University's 985 Project.

## References

- Acehan, D., Jiang, X., Morgan, D.G., Heuser, J.E., Wang, X., Akey, C.W., 2002. Three-dimensional structure of the apoptosome: implications for assembly, procaspase-9 binding, and activation. *Mol. Cell* 9, 423–432.
- Amarante-Mendes, G.P., Kim, N.C., Liu, L., Huang, Y., Perkins, C.L., Green, D.R., Bhalla, K., 1998. Bcr-Abl exerts its antiapoptotic effect against diverse apoptotic stimuli through blockage of mitochondrial release of cytochrome *c* and activation of caspase-3. *Blood* 91, 1700–1705.
- Bedi, A., Zehnauer, B.A., Barber, J.P., Sharkis, S.J., Jones, R.J., 1994. Inhibition of apoptosis by BCR-ABL in chronic myeloid leukemia. *Blood* 83, 2038–2040.
- Bedi, A., Barber, J.P., Bedi, G.C., El-Deiry, W.S., Sideransky, D., Vala, M.S., Akhtar, A., Hilton, J., Jones, R.J., 1995. BCR-ABL-mediated inhibition of apoptosis with delay of G2M transition after DNA damage: a mechanism of resistance to multiple anticancer agents. *Blood* 86, 1148–1158.
- Burapadaja, S., Bunchoo, A., 1995. Antimicrobial activity of tannins from *Terminalia citrina*. *Planta Med.* 61, 365–366.
- Cadenas, E., Davies, K.J.A., 2000. Mitochondrial free radical generation, oxidative stress, and aging. *Free Radical Biol. Med.* 29, 222–230.
- Gali, H.U., Perchellet, E.M., Klish, D.S., Johnson, J.M., Perchellet, J.P., 1992. Antitumor-promoting activities of hydrolyzable tannins in mouse skin. *Carcinogenesis* 13, 715–718.
- Gross, A., Jockel, J., Wei, M.C., Korsmeyer, S.J., 1998. Enforced dimerization of BAX results in its translocation, mitochondrial dysfunction and apoptosis. *EMBO J.* 17, 3878–3885.
- Hampton, M.B., Vanags, D.M., Porn-Ares, M.I., Orrenius, S., 1996. Involvement of extracellular calcium in phosphatidylserine exposure during apoptosis. *FEBS Lett.* 399, 277–282.
- Haslam, E., 1996. Natural polyphenols (vegetable tannins) as drugs: possible modes of action. *J. Nat. Prod.* 59, 205–215.
- Hockenbery, D.M., Oltvai, Z.N., Yin, X.-M., Millman, C.L., Korsmeyer, S.J., 1993. Bcl-2 functions in an antioxidant pathway to prevent apoptosis. *Cell* 75, 241–251.
- Ibrado, A.M., Huang, Y., Fang, G.F., Liu, L., Bhalla, K., 1996. Overexpression of Bcl-2 or Bcl-x(L) inhibits Ara-C-induced CPP32/Yama protease activity and apoptosis of human acute myelogenous leukemia HL-60 cells. *Cancer Res.* 56, 4743–4748.
- Kelso, G.F., Porteous, C.M., Coulter, C.V., Hughes, G., Porteous, W.K., Ledgerwood, E.C., Smith, R.A.J., Murphy, M.P., 2001. Selective targeting of a redox-active ubiquinone to mitochondria within cells—Antioxidant and antiapoptotic properties. *J. Biol. Chem.* 276, 4588–4596.
- Kroemer, G., Dallaporta, B., Resche-Rigon, M., 1998. The mitochondrial death/life regulator in apoptosis and necrosis. *Annu. Rev. Physiol.* 60, 619–642.
- Kuramochi-Motegi, A., Kuramochi, H., Kobayashi, F., Ekimoto, H., Takahashi, K., Kadota, S., Takamori, Y., Kikuchi, T., 1992. Woodfruticosin (woodfordin C), a new inhibitor of DNA topoisomerase II. Experimental antitumor activity. *Biochem. Pharmacol.* 44, 1961–1965.
- Li, P., Nijhawan, D., Budihardjo, I., Srinivasula, S.M., Ahmad, M., Alnemri, E.S., Wang, X., 1997. Cytochrome *c* and dATP-dependent formation of Apaf-1/caspase-9 complex initiates an apoptotic protease cascade. *Cell* 91, 479–489.
- Liu, X.S., Kim, C.N., Yang, J., Jemmerson, R., Wang, X.D., 1996. Induction of apoptotic program in cell-free extracts: requirement for dATP and cytochrome *c*. *Cell* 86, 147–157.
- Lubbert, M., Miller, C.W., Crawford, L., Koeffler, H.P., 1988. p53 in chronic myelogenous leukemia. Study of mechanisms of differential expression. *J. Exp. Med.* 167, 873–886.
- Lugo, T.G., Pendergast, A.M., Muller, A.J., Witte, O.N., 1990. Tyrosine kinase activity and transformation potency of *bcr-abl* oncogene products. *Science* 247, 1079–1082.
- Marchetti, P., Castedo, M., Susin, S.A., Zamzami, N., Hirsch, T., Macho, A., Haeflner, A., Hirsch, F., Geuskens, M., Kroemer, G., 1996. Mitochondrial permeability transition is a central coordinating event of apoptosis. *J. Exp. Med.* 184, 1155–1160.
- McConkey, D.J., Orrenius, S., 1997. The role of calcium in the regulation of apoptosis. *Biochem. Biophys. Res. Commun.* 239, 357–366.
- Miyamoto, K., Nomura, M., Murayama, T., Furukawa, T., Hatano, T., Yoshida, T., Koshiura, R., Okuda, T., 1993a. Antitumor activities of ellagitannins against sarcoma-180 in mice. *Biol. Pharm. Bull.* 16, 379–387.
- Miyamoto, K., Nomura, M., Sasakura, M., Matsui, E., Koshiura, R., Murayama, T., Furukawa, T., Hatano, T., Yoshida, T., Okuda, T., 1993b. Antitumor activity of Oenothien B, a unique macrocyclic ellagitannin. *Jpn. J. Cancer Res.* 84, 99–103.
- Mukhtar, H., Das, M., Khan, W.A., Wang, Z.Y., Bik, D.P., Bickers, D.R., 1988. Exceptional activity of tannic acid among naturally occurring plant phenols in protecting against 7,12-dimethylbenz(α)anthracene-, benzo(α)pyrene-, 3-methylcholanthrene-, and *N*-methyl-*N*-nitrosourea-induced skin tumorigenesis in mice. *Cancer Res.* 48, 2361–2365.
- Nakashima, H., Murakami, T., Yamamoto, N., Sakagami, H., Tanuma, S., Hatano, T., Yoshida, T., Okuda, T., 1992. Inhibition of human immunodeficiency viral replication by tannins and related compounds. *Antiviral Res.* 18, 91–103.
- Nicholson, D.W., Ali, A., Thornberry, N.A., Vaillancourt, J.P., Ding, C.K., Gallant, M., Gareau, Y., Griffin, P.R., Labelle, M., Lazebnik, Y.A., Munday, N.A., Raju, S.M., Smulson, M.E., Yamin, T.T., Yu, V.L., Miller, D.K., 1995. Identification and inhibition of the ICE/CED-3 protease necessary for mammalian apoptosis. *Nature* 376, 37–43.
- Polya, G.M., Wang, B.H., Foo, L.Y., 1995. Inhibition of signal-regulated protein kinases by plant-derived hydrolyzable tannins. *Phytochemistry* 38, 307–314.
- Ricci, J.E., Gottlieb, R.A., Green, D.R., 2003. Caspase-mediated loss of mitochondrial function and generation of reactive oxygen species during apoptosis. *J. Cell Biol.* 160, 65–75.
- Rosse, T., Olivier, R., Monney, L., Rager, M., Conus, S., Fellay, L., Jansen, B., Borner, C., 1998. Bcl-2 prolongs cell survival after Bax-induced release of cytochrome *c*. *Nature* 391, 496–499.

- Sakaguchi, N., Inoue, M., Ogihara, Y., 1998. Reactive oxygen species and intracellular  $\text{Ca}^{2+}$ , common signals for apoptosis induced by gallic acid. *Biochem. Pharmacol.* 55, 1973–1981.
- Sakahira, H., Enari, M., Nagata, S., 1998. Cleavage of CAD inhibitor in CAD activation and DNA degradation during apoptosis. *Nature* 391, 96–99.
- Satoh, K., Sakagami, H., 1996. Ascorbyl radical scavenging activity of polyphenols. *Anticancer Res.* 16, 2885–2890.
- Sawyers, C.L., Denny, C.T., Witte, O.N., 1991. Leukemia and the disruption of normal hematopoiesis. *Cell* 64, 337–350.
- Schlesinger, P.H., Gross, A., Yin, X.M., Yamamoto, K., Saito, M., Waksman, G., Korsmeyer, S.J., 1997. Comparison of the ion channel characteristics of proapoptotic BAX and antiapoptotic BCL-2. *Proc. Natl. Acad. Sci. U. S. A.* 94, 11357–11362.
- Simizu, S., Takada, M., Umezawa, K., Imoto, M., 1998. Requirement of caspase-3(-like) protease-mediated hydrogen peroxide production for apoptosis induced by various anticancer drugs. *J. Biol. Chem.* 273, 26900–26907.
- Thornberry, N.A., Rano, T.A., Peterson, E.P., Rasper, D.M., Timkey, T., Garcia-Calvo, M., Houtzager, V.M., Nordstrom, P.A., Roy, S., Vaillancourt, J.P., Chapman, K.T., Nicholson, D.W., 1997. A combinatorial approach defines specificities of members of the caspase family and granzyme B. Functional relationships established for key mediators of apoptosis. *J. Biol. Chem.* 272, 17907–17911.
- van Engeland, M., Nieland, L.J.W., Ramaekers, F.C.S., Schutte, B., Reutelingsperger, C.P.M., 1998. Annexin V-affinity assay: a review on an apoptosis detection system based on phosphatidylserine exposure. *Cytometry* 31, 1–9.
- Waterhouse, N.J., Goldstein, J.C., von Ahsen, O., Schuler, M., Newmeyer, D.D., Green, D.R., 2001. Cytochrome *c* maintains mitochondrial transmembrane potential and ATP generation after outer mitochondrial membrane permeabilization during the apoptotic process. *J. Cell Biol.* 153, 319–328.
- Wolter, K.G., Hsu, Y.T., Smith, C.L., Nechushtan, A., Xi, X.G., Youle, R.J., 1997. Movement of Bax from the cytosol to mitochondria during apoptosis. *J. Cell Biol.* 139, 1281–1292.
- Wood, D.E., Newcomb, E.W., 2000. Cleavage of Bax enhances its cell death function. *Exp. Cell Res.* 256, 375–382.
- Yang, J., Liu, X.S., Bhalla, K., Kim, C.N., Ibrado, A.M., Cai, J.Y., Peng, T.I., Jones, D.P., Wang, X.D., 1997. Prevention of apoptosis by Bcl-2: release of cytochrome *c* from mitochondria blocked. *Science* 275, 1129–1132.
- Yoshida, T., Chou, T., Haba, K., Okano, Y., Shingu, T., Miyamoto, K., Koshiura, R., Okuda, T., 1989. Camelliin B and Nobotanin I, Macrocyclic ellagitannin dimers and related dimers, and their antitumor activity. *Chem. Pharm. Bull.* 37, 3174–3176.
- Yoshida, T., Chou, T., Nitta, A., Okuda, T., 1992. Tannins and related polyphenols of Lythraceous Plants. III. Hydrozable tannin oligomers with macrocyclic structures, and accompanying tannins from *Woodfordia fruticosa* KURZ. *Chem. Pharm. Bull.* 40, 2023–2030.
- Yuan, Z.M., Huang, Y., Whang, Y., Sawyers, C., Weichselbaum, R., Kharbanda, S., Kufe, D., 1996. Role for c-Abl tyrosine kinase in growth arrest response to DNA damage. *Nature* 382, 272–274.
- Zamzami, N., Marchetti, P., Castedo, M., Zanin, C., Vayssiere, J.L., Petit, P.X., Kroemer, G., 1995. Reduction in mitochondrial potential constitutes an early irreversible step of programmed lymphocyte death in vivo. *J. Exp. Med.* 374, 1661–1672.
- Zamzami, N., Susin, S.A., Marchetti, P., Hirsch, T., GomezMonterrey, I., Castedo, M., Kroemer, G., 1996. Mitochondrial control of nuclear apoptosis. *J. Exp. Med.* 183, 1533–1544.